



## RESEARCH LETTER

10.1002/2015GL064604

## Key Points:

- Global rainfall fractions from liquid-phase, mixed-phase, and ice-phase clouds are derived
- Rain from liquid clouds over land is sharply reduced compared to oceans
- Smaller effective radii in continental warm clouds delay the onset of precipitation

## Supporting Information:

- Supporting Information S1
- Figure S1
- Figure S2
- Figure S3
- Figure S4
- Figure S5
- Figure S6
- Figure S7
- Figure S8

## Correspondence to:

J. Mülmenstädt,  
johannes.muellenstaedt@uni-leipzig.de

## Citation:

Mülmenstädt, J., O. Sourdeval, J. Delanoë, and J. Quaas (2015), Frequency of occurrence of rain from liquid-, mixed-, and ice-phase clouds derived from A-Train satellite retrievals, *Geophys. Res. Lett.*, 42, 6502–6509, doi:10.1002/2015GL064604.

Received 23 MAY 2015

Accepted 2 JUL 2015

Accepted article online 5 JUL 2015

Published online 6 AUG 2015

©2015. The Authors.

This is an open access article under the terms of the Creative Commons Attribution-NonCommercial-NoDerivs License, which permits use and distribution in any medium, provided the original work is properly cited, the use is non-commercial and no modifications or adaptations are made.

## Frequency of occurrence of rain from liquid-, mixed-, and ice-phase clouds derived from A-Train satellite retrievals

Johannes Mülmenstädt<sup>1</sup>, O. Sourdeval<sup>1</sup>, J. Delanoë<sup>2</sup>, and J. Quaas<sup>1</sup>

<sup>1</sup>Institute of Meteorology, Universität Leipzig, Leipzig, Germany, <sup>2</sup>Laboratoire Atmosphères, Milieux, Observations Spatiales (LATMOS UVSQ/CNRS/UPMC/IPSL), Guyancourt, France

**Abstract** A climatology of thermodynamic phase of precipitating cloud is presented derived from global—land and ocean—, retrievals from Cloudsat, CALIPSO, and Moderate Resolution Imaging Spectroradiometer. Like precipitation rate, precipitation frequency is dominated by warm rain, defined as rain produced via the liquid phase only, over the tropical oceans outside the Intertropical Convergence Zone and by cold rain, produced via the ice phase, over the midlatitude oceans and continents. Warm rain is very infrequent over the continents, with significant warm rain found only in onshore flow in the tropics, and over India, China, and Indochina. Comparison of the properties of precipitating and nonprecipitating warm clouds shows that the scarcity of warm rain over land can be explained by smaller effective radii in continental clouds that delay the onset of precipitation. The results highlight the importance of ice-phase processes for the global hydrological cycle and may lead to an improved parameterization of precipitation in general circulation models.

### 1. Introduction

*It was a dark and stormy night ...* That is the scenario under which we commonly perceive precipitation to be produced outside the tropics: in storm clouds where ice- or mixed-phase processes dominate condensate particle growth. Spaceborne precipitation and cloud radars aboard the Tropical Rainfall Measurement Mission (TRMM) and CloudSat satellites show that rain over the tropical oceans outside the Intertropical Convergence Zone (ITCZ) is predominantly from warm clouds, while rain over the midlatitude oceans is predominantly from ice clouds [Lau and Wu, 2003, 2011; Lebsock and L'Ecuyer, 2011]. However, to date, there is no global climatology of the thermodynamic phase of precipitating cloud over land and ocean.

In this paper, we use data from several satellites in the A-Train constellation to investigate what fraction of rain forms in liquid-phase (*warm*), mixed-phase, and ice-phase (*cold*) clouds. Only liquid-phase rain (including drizzle) is considered here, as we assume that solid precipitation (snow, hail, and graupel) always involves ice-phase processes; this assumption is discussed in section 4. As far as possible, the analysis relies on products that are available over land and ocean and retrieves the thermodynamic phase of the precipitating cloud without relying on temperature.

### 2. Data and Methods

Two pieces of information about clouds are required for this analysis. First, we need to know whether a cloud is raining. Rain identification is provided by the Cloud-Profiling Radar (CPR) aboard CloudSat [Stephens *et al.*, 2002]. Second, we need to know the thermodynamic phase at the height where the precipitation originates. We assume that if ice is present anywhere within the precipitating cloud column, the precipitation is due to the more efficient ice-phase processes rather than the less efficient liquid-phase process (collision-coalescence). Therefore, if the thermodynamic phase at cloud top—where it can be retrieved by satellite-borne instruments—is ice or mixed, we classify the precipitation as cold rain; if the thermodynamic phase at cloud top is liquid and no ice is detected below, we classify the precipitation as warm rain. The pieces of information required for the cloud top phase determination are available from a combination of CPR and the Cloud-Aerosol Lidar with Orthogonal Polarization (CALIOP) aboard CALIPSO [Winker *et al.*, 2009].

A typical raining cloud column used in this analysis has the following structure. A radar signal indicative of precipitation starts at some height above ground and then either continues to the ground or, for heavy rain,

attenuates before reaching the ground; precipitation that evaporates before reaching the ground is excluded from the analysis. Above this precipitation lies cloud identified by lidar backscatter, radar reflectivity, or both. Multiple further layers of cloud can lie atop the precipitating cloud layer; for some aspects of the analysis (comparison to Moderate Resolution Imaging Spectroradiometer (MODIS) cloud microphysical retrievals, and a sensitivity study), such columns are excluded. The cloud top phase determination is always made for the top of the lowest cloud layer above precipitation onset in the column. Cloud is identified by 2B-GEOPROF flag ( $\geq 30$ ) at 480 m resolution and interpolated onto the lidar vertical grid; if only part of a radar bin is occupied by cloud (because the cloud top does not coincide with a radar bin boundary) and CALIOP has not attenuated, then the part of the radar bin identified as clear by CALIOP (from the CALIOP vertical feature mask) is not counted as cloud. Possible biases resulting from cloud top phase misidentification due to higher cloud layers overlying the precipitating layer are addressed in section 4.

Rain is identified by CPR radar reflectivity. In this analysis, we use the 2C-PRECIP-COLUMN product [Haynes *et al.*, 2009, 2011] (version P1\_R04), which accounts for attenuation and multiple scattering of the radar beam and precipitation identification in the ground clutter region (the lowest five radar bins above the surface, approximately 1.2 km [Marchand *et al.*, 2008]). This analysis is restricted to rain that reaches the surface (2C-PRECIP-COLUMN precipitation flags “rain possible,” “rain probable,” and “rain certain”); it also excludes frozen or mixed-phase precipitation (since for these we assume that they always originate from cold processes), as flagged by 2C-PRECIP-COLUMN. Sensitivity of the results to the rain identification algorithm is discussed further in section 4.

Several methods for determining thermodynamic phase at cloud top exist. Ice particles and liquid droplets differ in their radar signature, with the ice particles reflecting more strongly than cloud droplets due to their larger size. In turn, large rain drops reflect microwave radiation more strongly than ice particles due to their higher dielectric constant. Ice and liquid particles also differ in their lidar signature, with more intense backscatter from liquid droplets due to the larger scattering cross section of the numerous small particles. We use the combined radar-lidar product DARDAR [Delanoë and Hogan, 2010; Ceccaldi *et al.*, 2013] (version DARDAR-MASK v1.1.4), where the combination of lidar backscatter and radar reflectivity is the basis for distinguishing between ice clouds, typical mixed-phase clouds where a liquid top overlies the ice, and liquid clouds. Additional information on cloud top phase is contained in the depolarization of the polarized CALIOP beam scattered from ice crystals [Hu *et al.*, 2007; Cesana and Chepfer, 2013]. Agreement between the DARDAR cloud top phase used in this analysis and depolarization-based retrieval algorithms is assessed in further detail in section 4.

Retrieving rain rate uniformly in warm and cold rain over land and ocean is a difficult task. While precipitation occurrence is determined both over land and over ocean by the CPR, operational products for retrieving precipitation intensity (2C-PRECIP-COLUMN and, specifically for warm rain, 2C-RAIN-PROFILE [Lebsock and L'Ecuyer, 2011]) exist only over ocean because they rely on a radar return from a surface with known radar backscatter cross section. Mitrescu *et al.* [2010] and Matrosov [2007, 2014] have developed experimental retrievals that do not depend on a known surface return, but these data sets are not operationally available. The TRMM precipitation radar [Kummerow *et al.*, 1998] also provides rain rate over land and ocean, but due to its longer wavelength it is less sensitive to drizzle [Short and Nakamura, 2000] than the CPR [e.g., Haynes *et al.*, 2009; Behrangi *et al.*, 2012] and is restricted to latitudes equatorward of 35°. The Global Precipitation Measurement mission now provides a TRMM-like product at higher latitudes, but has only been in orbit since 2014. Passive microwave retrievals of precipitation over land rely on scattering of microwave radiation by ice particles [e.g., Stephens and Kummerow, 2007] and are thus unsuitable for warm rain. We circumvent the difficulty of assembling a global precipitation rate climatology by instead analyzing rain occurrence, defining a rain event as liquid precipitation with an arbitrary intensity.

### 3. Results

In approximately 5 years of collocated CloudSat–CALIPSO data (2006–2011), we find slightly over 50 million raining profiles. Henceforth, we will refer to the fraction of raining columns with liquid-, mixed-, and ice-phase tops as the *phase fraction*, defined as

$$f_i(\lambda, \phi) = \frac{n_i(\lambda, \phi)}{\sum_i n_i(\lambda, \phi)}, \quad i \in \{\text{ice, liquid, mixed}\} \quad (1)$$

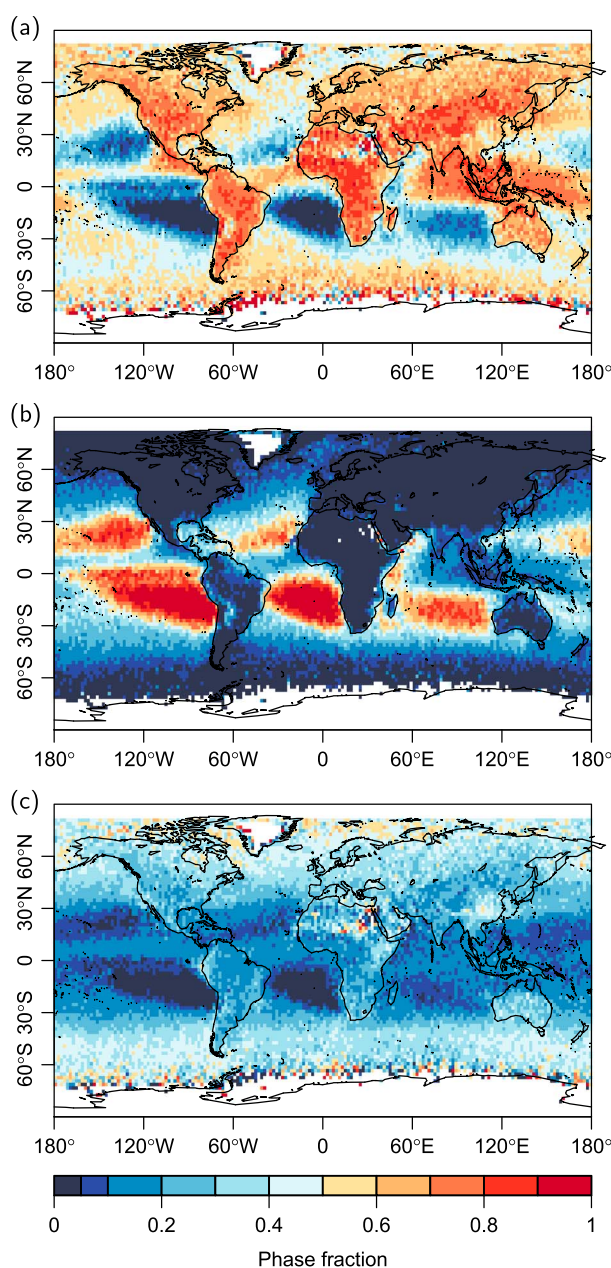


**Figure 1.** Fraction of raining clouds that are (a) ice phase, (b) liquid phase, and (c) mixed phase averaged over 5 years (2006–2011).

spheres just poleward of 30° latitude. Figures S7 and S8 in the supporting information show the phase fractions in each season (from which Figure 2 is calculated) and the geographic distribution of the seasonal differences.

Cold rain can be further subdivided into stratiform and convective precipitation based on the vertical profile of radar reflectivity. In stratiform precipitation, ice particles falling through the melting layer produce a band of high reflectivity (*bright band*) below which strong attenuation by rain drops occurs; in convective precipitation, updrafts can lift rain drops significantly above the freezing level, so that significant attenuation due to rain begins above the freezing level. The 2C-PRECIP-COLUMN product classifies the column as convective if the attenuation due to rain starts at least 500 m above the freezing level [Haynes et al., 2011]. The global annual mean fraction of raining columns classified as convective (and therefore the convective area fraction) is 10% for ice-phase, < 1% for liquid-phase, and 6% for mixed-phase raining clouds. The overall

where  $n_i(\lambda, \phi)$  is the number of raining columns with cloud top of phase  $i$  within the grid box at latitude  $\phi$  and longitude  $\lambda$ . (The cloud top phase in the case of multiple cloud layers refers to the phase at the top of the lowest layer above precipitation onset.) Figure 1 shows the phase fraction in each  $2^\circ \times 2^\circ$  latitude-longitude box. Like the warm rain amounts reported by Lau and Wu [2003] and Lebsock and L'Ecuyer [2011], the warm-rain phase fraction is highest in the tropical and subtropical oceans outside the ITCZ, where it is close to 100% over wide areas. In contrast, cold rain dominates in the ITCZ, over the midlatitude oceans, and in general over all continents. The fraction of raining columns with mixed-phase tops depends mainly on latitude, ranging from 10% over the tropical oceans to 30–50% at 60° north and south latitude, with higher values over the continents.

Figure 2 illustrates the strong seasonal variation of phase fraction. Compared to boreal winter, boreal summer sees a dramatic increase in cold rain over the northern tropics at the expense of warm rain, with a nearly symmetric increase in the southern tropics. The peak magnitude of the seasonal phase-fraction difference is 30% over ocean at 15°N, 40% over ocean at 15°S, and approximately 50% over land at 15° latitude in both hemispheres. This seasonal cycle follows the seasonal cycle of insolation. A weaker cycle of opposite sign and half the magnitude is observed over the midlatitude oceans. The midlatitude cycle could be due to destabilization of a cold air mass overlying a relatively warm ocean surface in winter. Finally, a seasonal difference in mixed-phase rain of approximately 10% exists in both hemi-

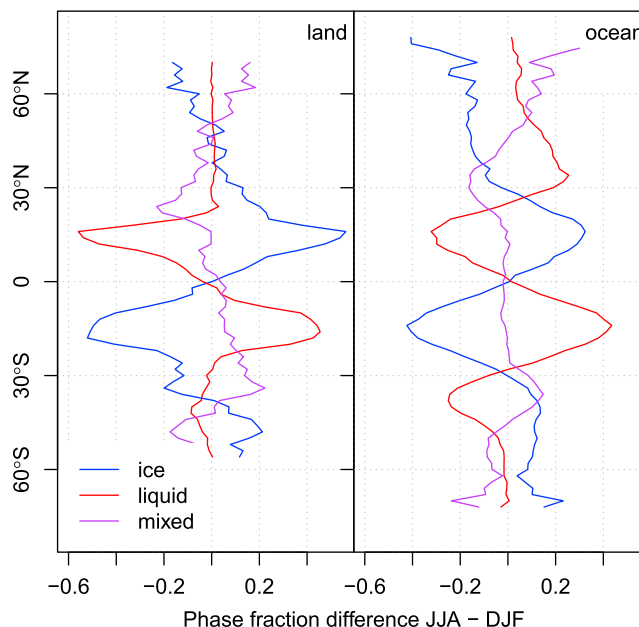


**Figure 2.** Difference between zonal mean phase fraction in December-January-February and June-July-August.

fraction of convective columns summed over the three cloud phases is 8%, in good agreement with Haynes *et al.* [2009].

Warm rain exhibits a remarkable land-sea contrast. Even at latitudes where rain from warm clouds is copious over ocean, there is almost no warm rain over land. Overall, the warm-rain phase fraction over land is only 1% in the extratropics (poleward of 30° latitude) and 8% in the tropics, while the warm-rain phase fraction over ocean is 15% in the extratropics and 44% in the tropics. (The ice-phase fractions are 67% and 71% over land in the extratropics and tropics; they are 50% and 45% over ocean in the extratropics and tropics. The remainder is mixed phase.) Rain from liquid clouds over land is mostly confined to regions of onshore flow in eastern South and Central America and Africa.

How can we explain the scarcity of warm rain over land? The continental and marine atmospheres differ in many respects that influence clouds, with less abundant moisture, higher aerosol concentrations, and greater turbulence production by surface heat fluxes that results in stronger updrafts over land. A land-sea contrast in warm-rain fraction is therefore not unexpected, even if its magnitude is surprising.

The presence of warm rain over continents in onshore flow can be explained as marine air masses that have not yet transitioned to continental. This explanation is supported by the gradient of warm-rain fraction as one moves downwind and onshore over the tropical continents. It is more difficult to explain the relative abundance of warm rain over southern Asia relative to other continental areas. A closer investigation of the individual warm-rain columns over India for 1 year (2008) shows that nearly 90% of single-layer columns also have a collocated MODIS cloud top temperature above 273 K, even though a sizable fraction of these warm clouds extend to 4–5 km height. This indicates that a combination of high surface temperature and sufficient moisture, rather than potential artifacts due to the presence of aerosol layers, is the cause of these continental warm-rain clouds.

It remains to be explained why warm rain is very infrequent also over the rest of the continents. The scarcity is the result of two factors. First, liquid clouds, raining or nonraining, make up a smaller fraction of DARDAR-observed clouds over land than over ocean (Figure 3a). Second, warm clouds over land are less likely to rain than warm clouds over ocean. Define the *rain probability* as

$$p_i(\lambda, \phi) = \frac{n_i(\lambda, \phi)}{N_i(\lambda, \phi)}, \quad i \in \{\text{ice, liquid, mixed}\} \quad (2)$$

with  $n_i(\lambda, \phi)$  the number of raining columns with cloud top phase  $i$  and  $N_i(\lambda, \phi)$  the number of DARDAR-observed cloud columns with cloud top phase  $i$  within the grid box at latitude  $\phi$  and longitude  $\lambda$ .

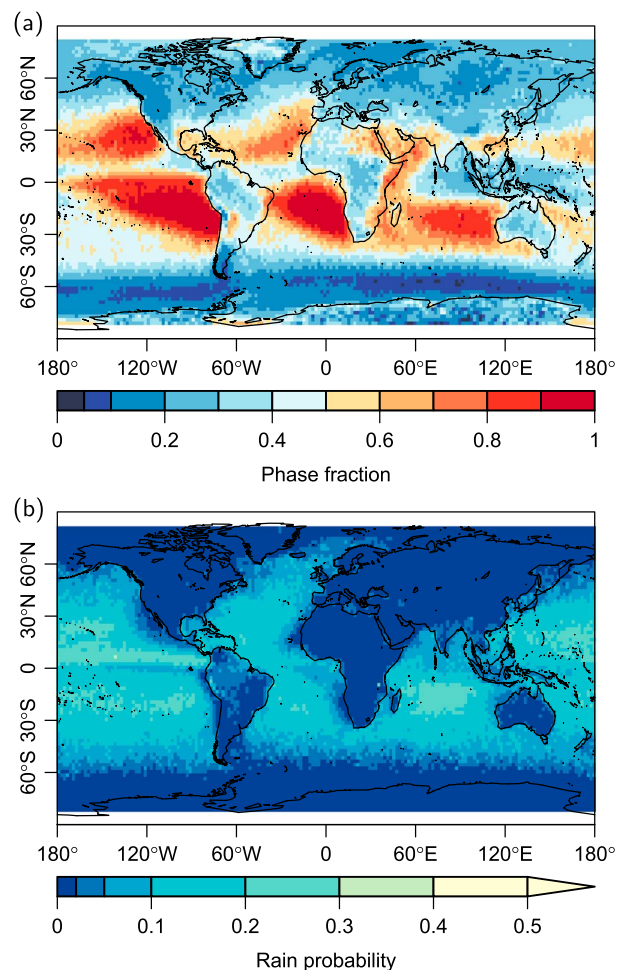


**Figure 3.** (a) Fraction of DARDAR-detected clouds that are liquid phase (see Figure S1 for ice-phase and mixed-phase cloud fractions). (b) Probability of precipitation of liquid DARDAR-detected clouds (See Figure S2 for the probabilities of precipitation of ice and mixed-phase clouds).

and higher tops than nonraining clouds. One explanation for the difference between marine and continental warm-rain probability consistent with these observations is that marine warm clouds are on average close to the  $r_e$  threshold for drizzle initiation [Freud and Rosenfeld, 2012] and require only a small perturbation to precipitate; continental clouds, on the other hand, have smaller effective radii, and greater vertical development is required before the cloud can precipitate. It is not possible to determine from these cloud variables whether the smaller effective radii of continental clouds are due to greater aerosol concentrations or due to more vigorous updrafts resulting in higher supersaturations.

#### 4. Assessment of Uncertainties

Uncertainties in the underlying satellite retrievals result in uncertainties and biases in the phase fractions. Warm rain is often drizzle, which is less likely to be detected; as a cloud radar, CPR is more sensitive to drizzle than precipitation radars, but a residual effect still exists. Temperature, taken from the interpolated meteorological analysis of the European Centre for Medium-Range Weather Prediction (ECMWF), the ECMWF-AUX data set, is mostly excluded as an error source by choosing algorithms that derive the cloud top phase from radiative signatures of liquid and ice-phase condensate. A residual dependence remains because no ice detection is attempted in clouds with an ECMWF-AUX cloud top wet-bulb temperature above freezing; we show below that this error is small. Land surface and sea surface differences in precipitation retrieval may bias the detection probability over land, but the assignment of cloud top phase is not sensitive to surface type. Where

(For both  $n_i$  and  $N_i$ , the cloud top phase in the case of multiple cloud layers refers to the phase at the top of the lowest layer.) While  $p_{ice}$  and  $p_{mixed}$  are slightly smaller over land than over ocean (see Figure S2), the occurrence reduction over land versus ocean is dramatic for  $p_{liquid}$ : the probability for rain from warm cloud is typically  $\geq 20\%$  over ocean but  $< 2\%$  over land (Figure 3b).

To understand this lower warm-rain probability, we next investigate the differences in liquid water content (LWC), effective radius ( $r_e$ ), and cloud top height ( $z_{top}$ ) between continental and marine raining and nonraining CloudSat-detected warm clouds. For the daytime portions of 1 year of data (2008), the MODIS Collection 6 cloud product cloud top effective radius, and cloud liquid water content were collocated to the CloudSat track. Only profiles identified as single-layer by DARDAR were used so as to avoid artifacts from multilayer MODIS retrievals; approximately 40% of profiles satisfy this requirement. Due to the reduced number of observations, the cloud variables are aggregated to 5° latitude zonal bands over land and ocean; latitude bands with fewer than 100 observations (near the poleward edge of rain occurrence) are not used. The distributions are shown in Figure 4. Over ocean, the effective radius and cloud top height of raining and nonraining clouds are similar, while over land raining clouds have larger effective radius

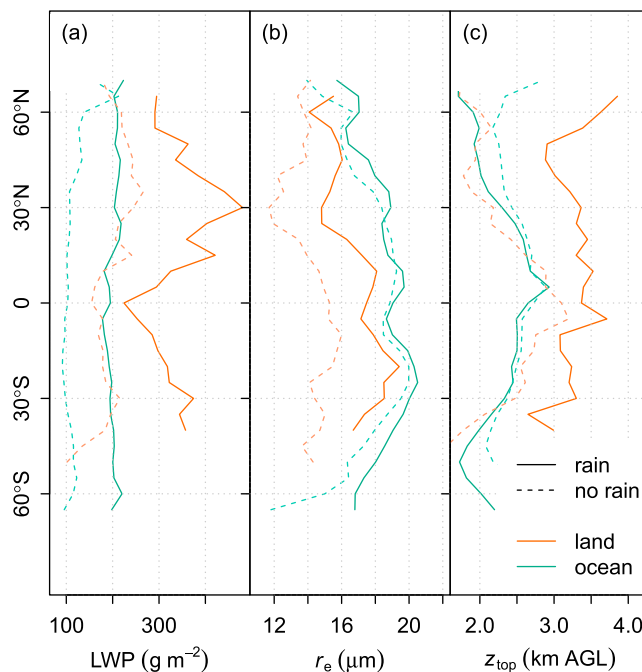


**Figure 4.** Cloud properties of raining and nonraining single-layer liquid CloudSat cloud columns over land and ocean. (a) MODIS geometric mean liquid water path, (b) MODIS geometric mean effective radius, and (c) DARDAR mean cloud top height above ground.

a gradual transition occurs between high warm-rain fraction over ocean and low warm-rain fraction over land, the transition region often includes one or more  $2^\circ \times 2^\circ$  latitude-longitude boxes with elevated warm-rain fraction that are entirely over land, demonstrating that the land-sea contrast cannot be entirely due to algorithmic differences.

Atmospheric columns with multiple cloud layers, in particular cirrus clouds overlying raining warm clouds, are common [Haynes and Stephens, 2007]. The thermodynamic phase assigned to the raining cloud is the phase at the top of the lowest cloud layer above precipitation onset. In scenes with multiple cloud layers, it is possible that cloud layers merge and the top of the wrong cloud is used to determine thermodynamic phase. This could be the case, for example, in a seeder-feeder situation where ice crystals sediment through clear air from an ice cloud into a liquid cloud at lower altitude, and the radar sensitivity to ice crystals leads to the clear air layer being classified as cloud; this type of misidentification is actually beneficial, since the precipitation forms through an ice-phase process. It is also possible that a single cloud layer is spuriously split in two because the radar reflectivity falls below the single-column detection limit. However, we do not expect a large cloud-phase misidentification probability from such spuriously split columns, as both the liquid and the ice parts of the column will contain large targets (ice particles or rain drops) with high reflectivity. To test whether our results are robust to potential layer misidentification, we have repeated the analysis exclusively for single-layer columns, i.e., columns in which neither radar nor lidar detects another cloud layer above the precipitating layer. This results in a higher ice-cloud phase fraction, mostly at the expense of mixed-phase clouds but also at the expense of warm clouds, as shown in Figure S3; presumably this is because the top of ice clouds is higher, reducing the likelihood for another layer. The conclusions of the paper are not qualitatively different when considering only single-layer clouds (compare Figures 1 and S3).

To assess the robustness of our results against retrieval errors and uncertainties, we compare the rain identification and cloud top phase identification algorithms used in this analysis against other retrieval algorithms applied to the CPR and CALIOP profiles. These comparisons show good agreement, increasing our confidence in the results. Phase misidentification effects can be estimated by comparing the DARDAR and the general circulation model-oriented CALIPSO cloud product (GOCCP) instant scattering ratio phase [Cesana and Chepfer, 2013] phase retrieval methods. DARDAR relies on a comparison of radar and lidar intensity profiles, while GOCCP uses depolarization of polarized incident lidar by ice crystals (which, however, requires vertical averaging and thus reduces the vertical resolution compared to DARDAR). The global average disagreement

between the two methods is 5% for ice-topped and 1% for liquid-topped (phases according to the DARDAR classification) clouds, with no strong regional variation.

To test the possibility that the conclusions of our analysis might change if we were to consider lighter drizzle or precipitation that evaporates before reaching the ground, we compare the results to a version of the analysis that uses the DARDAR precipitation flag in place of the 2C-PRECIP-COLUMN flag. The reflectivity threshold for drizzle identification is lower in the DARDAR precipitation flag ( $-17$  dBZ instead of  $-15$  dBZ), and precipitation is not required to continue to the ground. Figure S4 shows the resulting phase fractions, which lead to the same conclusion of very infrequent of warm rain over land, although not quite as infrequent as when using the 2C-PRECIP-COLUMN precipitation flag. The interpretation is that warm-phase light drizzle formation occurs at relatively larger frequency over land. This interpretation is supported by considering the 2C-PRECIP-COLUMN rain flags—rain certain, rain probable, and rain possible—separately (Figure S5). The rain possible flag, where the lightest drizzle detected by 2C-PRECIP-COLUMN would be found, shows greater warm-rain occurrence fraction over land than the rain certain and rain probable flags.

We expect that liquid cloud processes do not contribute to solid precipitation. To test this expectation, we calculate the phase fractions of precipitating columns identified as mixed precipitation (rain and ice) or snow at the surface by 2C-PRECIP-COLUMN (Figure S6). Mixed precipitation (“mixed precipitation possible” and “mixed precipitation certain”) behaves as expected, with negligible contributions from liquid-phase clouds. Snow (“snow possible” and “snow certain”) has a surprisingly high liquid cloud occurrence fraction in the polar regions and over Siberia, far exceeding the warm-rain fraction; this is true even when only snow certain columns are considered. It is conceivable that a liquid cloud above a colder layer of air could produce solid or mixed precipitation at the surface. However, it seems physically unlikely that snow would have a larger fraction of occurrence from liquid clouds than rain, so this is presumably an artifact. When all types of precipitation are considered together, our conclusion that very little precipitation over the extratropical continents originates in liquid-phase clouds is unchanged except over Antarctica, Siberia, and arctic North America, as shown in Figure S6c.

#### Acknowledgments

This study was supported by the European Union in an ERC starting grant (“QUAERERE,” grant agreement 306284) and a collaborative project (MACC-II, grant agreement 218793, FP7, and its successor project, MACC-III, grant agreement 633080, Horizon2020). We thank the NASA CloudSat project and the CloudSat Data Center for providing access to the 2B-CLDCLASS, 2C-COLUMN-PRECIP, and 2B-GEOPROF data, and the GOCCP project for access to the GOCCP Instant SR Phase product. The MODIS Collection 6 data used in this study were acquired as part of NASA’s Earth-Sun System Division and archived and distributed by the MODIS Adaptive Processing System (MODAPS). We thank the ICARE Data and Services Center for providing access to the DARDAR, CloudSat, and MODIS Collection 6 data used in this study. All data sets used in the analysis are freely available at <http://www.icare.univ-lille1.fr/archive> and [http://climserv.ipsl.polytechnique.fr/cfmip-obs/Calipso\\_goccp.html](http://climserv.ipsl.polytechnique.fr/cfmip-obs/Calipso_goccp.html). We thank three anonymous reviewers for comments that led to improvements in the analysis and clarifications in the text. The analysis was performed in R [R Core Team, 2012].

The Editor thanks two anonymous reviewers for their assistance in evaluating this paper.

## 5. Conclusions and Outlook

This paper presents the global—land and ocean—climatology of rain occurrence fraction from ice-, liquid-, and mixed-phase cloud as derived from satellite retrievals. The results of *Lau and Wu* [2003] and *Lebsock and L’Ecuyer* [2011] for rain rate over ocean are found to hold for rain frequency of occurrence: large contributions by warm rain over the tropical oceans outside the ITCZ and smaller contributions over the midlatitude oceans. Over wide areas in the tropical oceans, warm rain accounts for close to 100% of rain occurrences. This pattern tracks the seasonal pattern of insolation closely.

The most striking feature of the phase fraction is the very infrequent occurrence of warm rain over land compared to ocean. Appreciable amounts of rain from liquid-phase clouds over land occur near coasts in onshore flow and over much of southern Asia. Which of the differences between the continental and maritime atmosphere—less abundant moisture, stronger updrafts, higher aerosol concentrations, or greater variability of surface heat fluxes over land—is responsible for this contrast could not be determined. Further investigation of this question could improve our understanding of precipitation formation mechanisms and also may help test hypotheses on the role of aerosol-cloud interactions in precipitation.

General circulation models are biased in rain frequency and intensity [e.g., *Dai*, 2006; *Stephens et al.*, 2010; *Nam and Quaas*, 2012]. By providing additional observational constraints on relative frequency of precipitation from warm and cold processes, which favor drizzle and heavy precipitation, respectively, our results may prove of use in improving precipitation parameterization in models. Finally, our results highlight the importance of ice- and mixed-phase cloud processes in the hydrological cycle outside the tropical oceans.

## References

- Behrangi, A., M. Lebsock, S. Wong, and B. Lambriksen (2012), On the quantification of oceanic rainfall using spaceborne sensors, *J. Geophys. Res.*, *117*, D20105, doi:10.1029/2012JD017979.
- Ceccaldi, M., J. Delanoë, R. J. Hogan, N. L. Pounder, A. Protat, and J. Pelon (2013), From CloudSat-CALIPSO to EarthCare: Evolution of the DARDAR cloud classification and its comparison to airborne radar-lidar observations, *J. Geophys. Res. Atmos.*, *118*, 7962–7981, doi:10.1002/jgrd.50579.
- Cesana, G., and H. Chepfer (2013), Evaluation of the cloud thermodynamic phase in a climate model using CALIPSO-GOCCP, *J. Geophys. Res. Atmos.*, *118*(14), 7922–7937, doi:10.1002/jgrd.50376.

- Dai, A. (2006), Precipitation characteristics in eighteen coupled climate models, *J. Clim.*, *19*(18), 4605–4630, doi:10.1175/JCLI3884.1.
- Delanoë, J., and R. J. Hogan (2010), Combined CloudSat-CALIPSO-MODIS retrievals of the properties of ice clouds, *J. Geophys. Res.*, *115*, D00H29, doi:10.1029/2009JD012346.
- Freud, E., and D. Rosenfeld (2012), Linear relation between convective cloud drop number concentration and depth for rain initiation, *J. Geophys. Res.*, *117*, D02207, doi:10.1029/2011JD016457.
- Haynes, J. M., and G. L. Stephens (2007), Tropical oceanic cloudiness and the incidence of precipitation: Early results from CloudSat, *Geophys. Res. Lett.*, *34*, L09811, doi:10.1029/2007GL029335.
- Haynes, J. M., T. S. L'Ecuyer, G. L. Stephens, S. D. Miller, C. Mitrescu, N. B. Wood, and S. Tanelli (2009), Rainfall retrieval over the ocean with spaceborne W-band radar, *J. Geophys. Res.*, *114*, D00A22, doi:10.1029/2008JD009973.
- Haynes, J. M., T. L'Ecuyer, D. Vane, G. Stephens, and D. Reinke (2011), Level 2-C Precipitation Column Algorithm Product Process Description and Interface Control Document, paper presented at CloudSat Data Processing Center, Colo. State Univ., Fort Collins, Colo., 22 Jan. [Available at [http://www.cloudsat.cira.colostate.edu/sites/default/files/products/files/2C-PRECIP-COLUMN\\_PDICD.P1\\_R04.20110818.pdf](http://www.cloudsat.cira.colostate.edu/sites/default/files/products/files/2C-PRECIP-COLUMN_PDICD.P1_R04.20110818.pdf).]
- Hu, Y., M. Vaughan, C. McClain, M. Behrenfeld, H. Maring, D. Anderson, S. Sun-Mack, D. Flittner, J. Huang, B. Wielicki, P. Minnis, C. Weimer, C. Trepte, and R. Kuehn (2007), Global statistics of liquid water content and effective number concentration of water clouds over ocean derived from combined CALIPSO and MODIS measurements, *Atmos. Chem. Phys.*, *7*(12), 3353–3359, doi:10.5194/acp-7-3353-2007.
- Kummerow, C., W. Barnes, T. Kozu, J. Shiue, and J. Simpson (1998), The Tropical Rainfall Measuring Mission (TRMM) sensor package, *J. Atmos. Oceanic Technol.*, *15*(3), 809–817, doi:10.1175/1520-0426(1998)015<0809:TRMMT>2.0.CO;2.
- Lau, K. M., and H. T. Wu (2003), Warm rain processes over tropical oceans and climate implications, *Geophys. Res. Lett.*, *30*(24), 2290, doi:10.1029/2003GL018567.
- Lau, K.-M., and H.-T. Wu (2011), Climatology and changes in tropical oceanic rainfall characteristics inferred from Tropical Rainfall Measuring Mission (TRMM) data (1998–2009), *J. Geophys. Res.*, *116*, D17111, doi:10.1029/2011JD015827.
- Lebsock, M. D., and T. S. L'Ecuyer (2011), The retrieval of warm rain from CloudSat, *J. Geophys. Res.*, *116*, D20209, doi:10.1029/2011JD016076.
- Marchand, R., G. G. Mace, T. Ackerman, and G. Stephens (2008), Hydrometeor detection using CloudSat—An earth-orbiting 94-GHz cloud radar, *J. Atmos. Oceanic Technol.*, *25*(4), 519–533, doi:10.1175/2007JTECHA1006.1.
- Matrosov, S. Y. (2007), Potential for attenuation-based estimations of rainfall rate from CloudSat, *Geophys. Res. Lett.*, *34*, L05817, doi:10.1029/2006GL029161.
- Matrosov, S. Y. (2014), Intercomparisons of CloudSat and ground-based radar retrievals of rain rate over land, *J. Appl. Meteorol. Climatol.*, *53*(10), 2360–2370, doi:10.1175/JAMC-D-14-0055.1.
- Mitrescu, C., T. L'Ecuyer, J. Haynes, S. Miller, and J. Turk (2010), CloudSat precipitation profiling algorithm-model description, *J. Appl. Meteorol. Climatol.*, *49*(5), 991–1003, doi:10.1175/2009JAMC2181.1.
- Nam, C. C. W., and J. Quaas (2012), Evaluation of clouds and precipitation in the ECHAM5 general circulation model using CALIPSO and CloudSat satellite data, *J. Clim.*, *25*(14), 4975–4992, doi:10.1175/JCLI-D-11-00347.1.
- R Core Team (2012), *R: A Language and Environment for Statistical Computing*, R Foundation for Statistical Computing, Vienna, Austria.
- Short, D. A., and K. Nakamura (2000), TRMM radar observations of shallow precipitation over the tropical oceans, *J. Clim.*, *13*(23), 4107–4124, doi:10.1175/1520-0442(2000)013<4107:TROOSP>2.0.CO;2.
- Stephens, G. L., and C. D. Kummerow (2007), The remote sensing of clouds and precipitation from space: A review, *J. Atmos. Sci.*, *64*(11), 3742–3765, doi:10.1175/2006JAS2375.1.
- Stephens, G. L., et al. (2002), The CloudSat mission and the A-Train—A new dimension of space-based observations of clouds and precipitation, *Bull. Am. Meteorol. Soc.*, *83*(12), 1771–1790, doi:10.1175/BAMS-83-12-1771.
- Stephens, G. L., T. L'Ecuyer, R. Forbes, A. Gettleman, J.-C. Golaz, A. Bodas-Salcedo, K. Suzuki, P. Gabriel, and J. Haynes (2010), Dreary state of precipitation in global models, *J. Geophys. Res.*, *115*, D24211, doi:10.1029/2010JD014532.
- Winker, D. M., M. A. Vaughan, A. Omar, Y. Hu, K. A. Powell, Z. Liu, W. H. Hunt, and S. A. Young (2009), Overview of the CALIPSO mission and CALIOP data processing algorithms, *J. Atmos. Oceanic Technol.*, *26*(11), 2310–2323, doi:10.1175/2009JTECHA1281.1.